

MERIDIONAL FLOWS FROM RING DIAGRAM ANALYSIS

I. GONZÁLEZ HERNÁNDEZ AND J. PATRÓN

Instituto de Astrofísica de Canarias, 38200 La Laguna, Tenerife, Spain; iglez@ll.iac.es, jpr@ll.iac.es

R. S. BOGART

Stanford University, Center for Space Science and Astrophysics, HEPL A202, Stanford, California; rbogart@solar.stanford.edu

AND

THE SOI RING DIAGRAM TEAM

Received 1998 August 27; accepted 1998 November 6; published 1998 December 17

ABSTRACT

In order to search for meridional circulation in the solar envelope, we have applied *ring diagram analysis* to a set of small regions over the surface. The helioseismic data consist of Solar Oscillation Investigation/Michelson Doppler Imager Dopplergrams taken over a time span of about 50 hr (~3000 images) on 1998 June 20–22. The regions studied cover 115° in latitude centered on the equator and 30° in longitude. We find poleward flows between $r/R_\odot = 0.97$ and the surface. There is no evidence in this depth range for the return path of these meridional flows. The temporal stability of these flows will be discussed after the analysis of a synoptic map obtained using the same technique.

Subject headings: convection — Sun: oscillations

1. INTRODUCTION

Meridional flows, large-scale mass motions from the equator to the poles, are one of the few global-scale motions in the Sun, together with the differential rotation, for which there exists observational evidence (Arévalo et al. 1982; Pérez Gardé 1979). Most work up to now has been based on surface tracers such as sunspots or other magnetic features, and the results are very controversial.

The ring diagram analysis method (Hill 1988) is a local helioseismology technique for obtaining information about motions in the upper layers of the solar convection zone (Patrón et al. 1995). By studying local regions on the solar surface, in which curvature can be neglected, it is possible to construct three-dimensional power spectra ($k_x - k_y - \omega$) of medium–high degree ($0.3 \text{ Mm}^{-1} \lesssim k$) solar acoustic modes. Cuts of such diagrams at specific temporal frequencies show the power to be concentrated in sets of concentric rings, from which the name of the method is derived. Each ring corresponds to a particular value of the radial order n .

A horizontal velocity field present in the region in which the modes propagate produces an advection effect of the wave front and a shift in the frequencies of the modes, $\Delta\omega = \mathbf{k}_n \cdot \mathbf{U}_n$. Such a displacement manifests itself as an effective displacement of the centers of the rings in the constant frequency cuts.

By fitting the measured three-dimensional power spectrum of a region to a model that takes into account the frequency shift due to the velocity field, we recover the components U_x and U_y of the horizontal velocity flows as a function of frequency for each n . These functions are then inverted with respect to a kernel embodying the known thermal structure to obtain the velocities as a function of depth. To study the meridional flows, we isolate the latitudinal component (U_y) of the flows.

2. THE METHOD

To obtain the horizontal velocities as a function of depth, we proceed through several steps. First, a time series of Dopplergrams of the region under study is needed to obtain infor-

mation about the temporal frequency of the modes. To eliminate the gross advection due to solar rotation, the selected region is tracked with a model for the photospheric differential rotation: $\Omega = a_0 - a_2 \cdot \cos^2(\phi) - a_4 \cdot \cos^4(\phi) - s_0$, where ϕ is the colatitude of the center of the region and $s_0 = 31.7 \text{ nHz}$ is the sidereal-to-synodic correction. We use the a_i coefficients given by Snodgrass (1984: $a_0 = 452.0$, $a_2 = 49.0$, and $a_4 = 84.0 \text{ nHz}$), appropriate for the photospheric plasma rate. Since our attention is limited to medium–high degree modes in small regions near the center of the solar disk, the mode amplitudes can be decomposed with a plane-wave approximation instead of the typical spherical harmonic decomposition. To do this, we first map the data onto a plane in an azimuthal equidistant projection, which has been shown to be the most appropriate coordinate system for the plane-wave approximation (Haber et al. 1995).

The mapped time series data are Fourier transformed in both the spatial and temporal directions to obtain the three-dimensional power spectra. The spectra are then fitted to a ring model (described in Patrón 1994), which takes account of the shifts produced by the horizontal velocity field. The components of the horizontal velocity, U_x and U_y (as well as several other parameters concerning amplitudes, widths, background, and unperturbed positions of the peaks), are recovered as fit parameters for each temporal frequency and specific n value.

The final step is an inversion to obtain the dependence of the velocities with depth. The method is based on a least-squares piecewise constant fit with second-derivative smoothing. The set of kernels used for the inversions was derived from a standard solar model by Bahcall & Ulrich (1988). The method was developed by F. Hill and D. Gough and has been tested in previous applications of ring diagram analysis (González Hernández 1998a). A detailed description of the method is given in González Hernández et al. (1998c).

3. APPLICATION TO SOI/MDI DATA

In order to limit the scope of the investigation to small regions and to comparatively high-degree modes, for which the plane-wave approximation is justified, it is necessary to use high-resolution helioseismic data. The Solar Oscillation Inves-

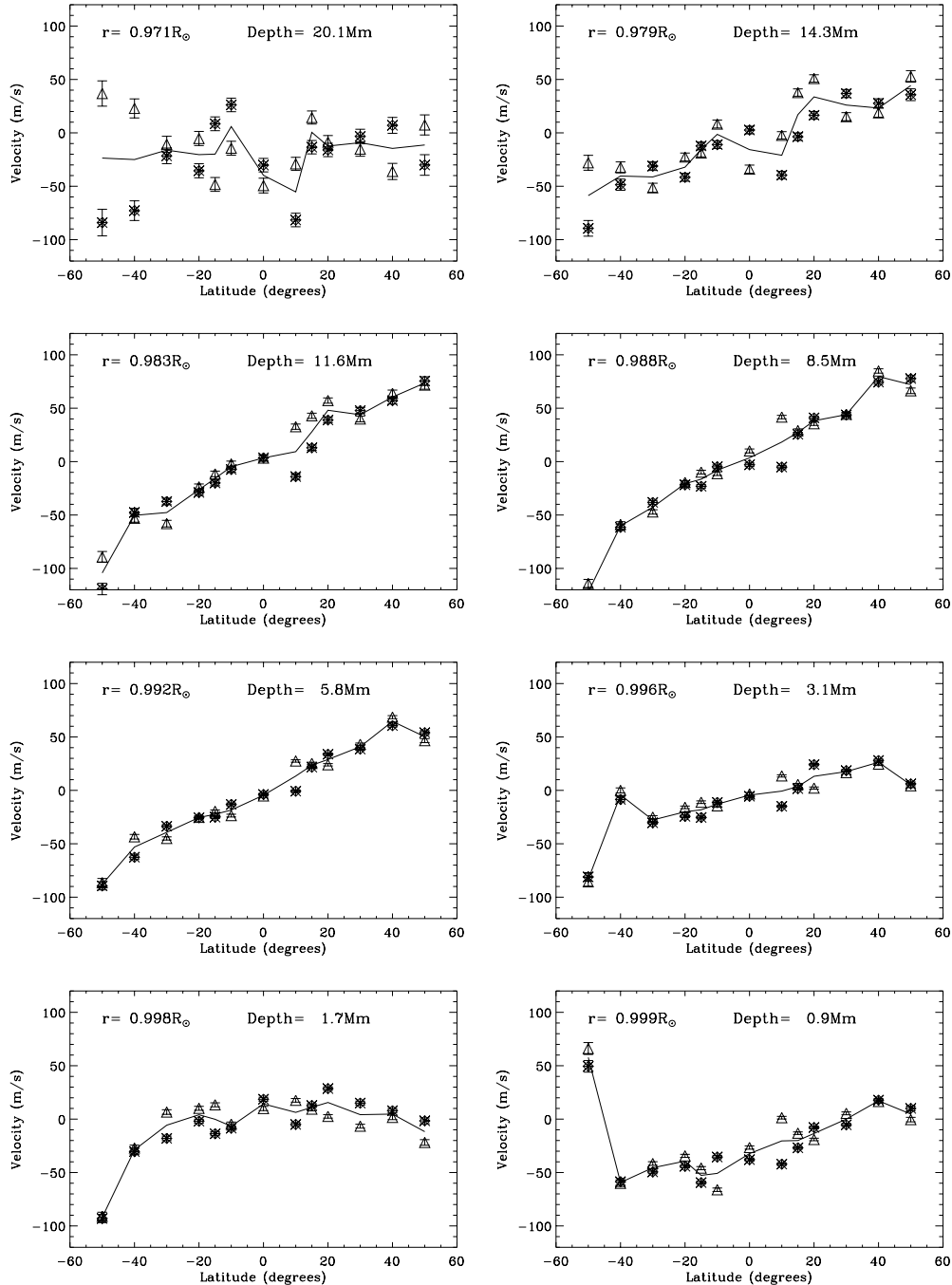


FIG. 1.—Meridional component (U_x) of the horizontal velocity flows at different latitudes. The lines show the average results of the two longitudes at different depths. Velocities for the individual longitudes are plotted as triangles (90°) and asterisks (105°).

tigation/Michelson Doppler Imager (SOI/MDI) on board the *Solar and Heliospheric Observatory* provides full-disk Dopplergrams with a resolution of $\sim 2'' \text{ pixel}^{-1}$ every minute during its Dynamic Program for 2–3 months each year (Scherrer et al. 1995). In this work, we used SOI/MDI images taken during the period 1996 June 20–22.

We studied two groups of 13 regions, each about $15^\circ \times 15^\circ$ in extent. The regions in each group were centered at latitudes 0° , $\pm 10^\circ$, $\pm 15^\circ$, $\pm 20^\circ$, $\pm 30^\circ$, $\pm 40^\circ$, and $\pm 50^\circ$. The two groups were centered on Carrington longitudes 90° and 105° , respectively, of Carrington rotation number 1910. There is thus substantial overlap in latitude of the various regions,

but none in longitude between the two groups. The time span of each series is 1536 ± 768 minutes from the time of its central meridian crossing. This minimizes the projection effects.

After tracking, mapping, and transforming these sections as described above, we obtain three-dimensional spectra with a spatial frequency resolution of $3.37 \times 10^{-2} \text{ Mm}^{-1}$ and a temporal frequency resolution of $10.85 \mu\text{Hz}$.

The fitting procedure normally fits two radial orders n at a time, with a total of 12 free parameters. We fit only the first spectra of the whole set with this method; the rest of the regions were fit with a four-parameter model in which only U_x^n and

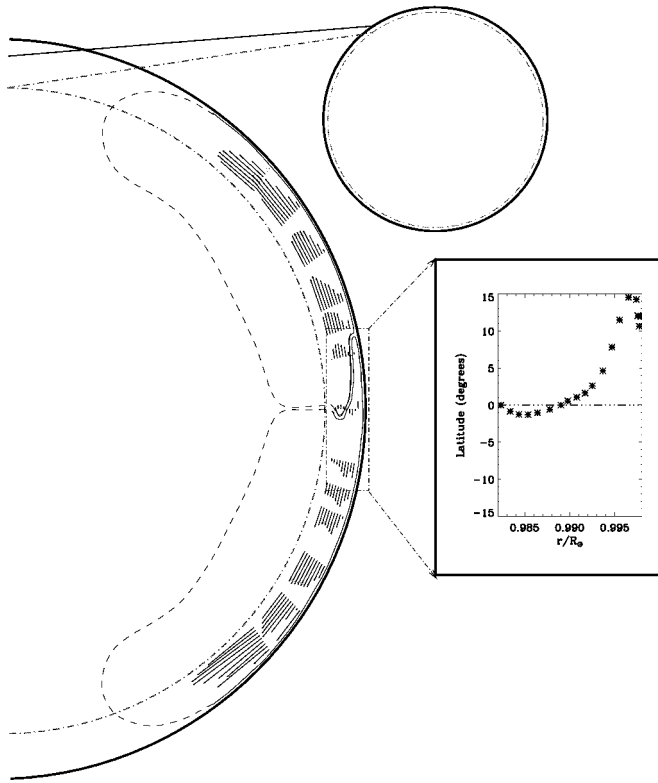


FIG. 2.—Plot of the meridional flows obtained as the average of the U_y components of the two sections located at the same latitude (0° , $\pm 10^\circ$, $\pm 15^\circ$, $\pm 20^\circ$, $\pm 30^\circ$, $\pm 40^\circ$, and $\pm 50^\circ$). Velocity vectors have been interpolated in depth to produce the plot. The plot on the right shows the latitude at which the velocity flows are estimated to diverge as a function of depth.

U_y^n are allowed to vary, while the rest of the parameters are assumed to be the same as those obtained for the first spectrum. The results of the fits for these parameters using both methods for the same regions are in exact agreement to within the error bars (González Hernández 1998a).

A total of 1536 modes with $0 \leq n \leq 7$ and $183 \leq l \leq 999$ ($l = k R_\odot$) have been used in the inversion procedure. This range theoretically permits inversion over a depth range from $r = 0.95 R_\odot$ to the surface.

4. MERIDIONAL FLOWS

By applying the ring diagram analysis method to the 26 sections described above, we obtained the average horizontal velocities U_x and U_y as a function of depth in a range of about $0.97 R_\odot$ to the surface for each region. The inferred flows below this depth appear to be completely disorganized. To study the meridional flows, we isolated the latitudinal component U_y . In Figure 1 we show the results at different depths for each longitude (triangles and asterisks) and for the 13 sections at different latitudes. The average of the two sections at the same latitude is also plotted.

Below $0.979 R_\odot$, the velocity flows are apparently chaotic, but there is a remarkable meridional behavior of those flows between 0.979 and $0.999 R_\odot$. At these depths the velocities are predominantly poleward. Above this region and up to the surface, the flows appear again to be disorganized. Figure 2 helps to visualize the meridional flows. The vectors have been interpolated in depth. The plot on the right shows the approximate latitude at each depth where the matter diverges toward the poles. This position has been estimated using a linear fit to determine the position in latitude of $V_y = 0$ for every depth, which works well for almost the entire depth range but fails at the surface, where the behavior of the flows is chaotic.

To study the temporal behavior of the meridional flows, we averaged the latitudinal components (U_y) of 24 sections in longitude situated at latitudes 0° , $\pm 15^\circ$, and $\pm 30^\circ$ of a synoptic map obtained using the same technique (González Hernández et al. 1998b), covering 360° in longitude over a total elapsed time corresponding to a solar rotation. The results are displayed in Figure 3, in which they are compared with those for only two longitudes but spread out in latitude.

5. CONCLUSIONS

Our results provide clear evidence that meridional circulation exists and that material is flowing from the equator to the poles between 0.97 and $0.999 R_\odot$. We do not find a return flow from the poles to the equator in the range of depth studied, suggesting that it takes place at a deeper layer. Near the surface the flows become disorganized, which could explain the diversity of results obtained with other techniques relying on surface observations. The latitudes at which the material diverges toward each pole are localized around the equator, but vary somewhat with depth. This may be related to the shape of the meridional cells.

The averages over all sections located at the same latitude in the synoptic map (González Hernández et al. 1998b) show that the flows are very stable in both time and space. The stability of this axisymmetric component of the meridional flows extends to greater depths, reaching a zone of about $0.97 R_\odot$. At this depth the amplitude of the velocity has decreased considerably, suggesting that it may be close to the point of reversal of the meridional flows between the poles and the equator.

We thank Teodoro Roca Cortés for his help and advice during the preparation of this Letter. The entire work has been performed at the headquarters of the Instituto de Astrofísica de Canarias. Part of the reduction process was carried out on the Jet Propulsion Laboratory Caltech Cray supercomputer. The supercomputer used in this investigation was provided by funding from the NASA offices of Mission to Planet Earth, Aeronautics, and Space Science.

The Solar Oscillations Investigation—Michelson Doppler Imager project on *SOHO* is supported by NASA grant NAS5-3077 at Stanford University. *SOHO* is a project of international cooperation between ESA and NASA.

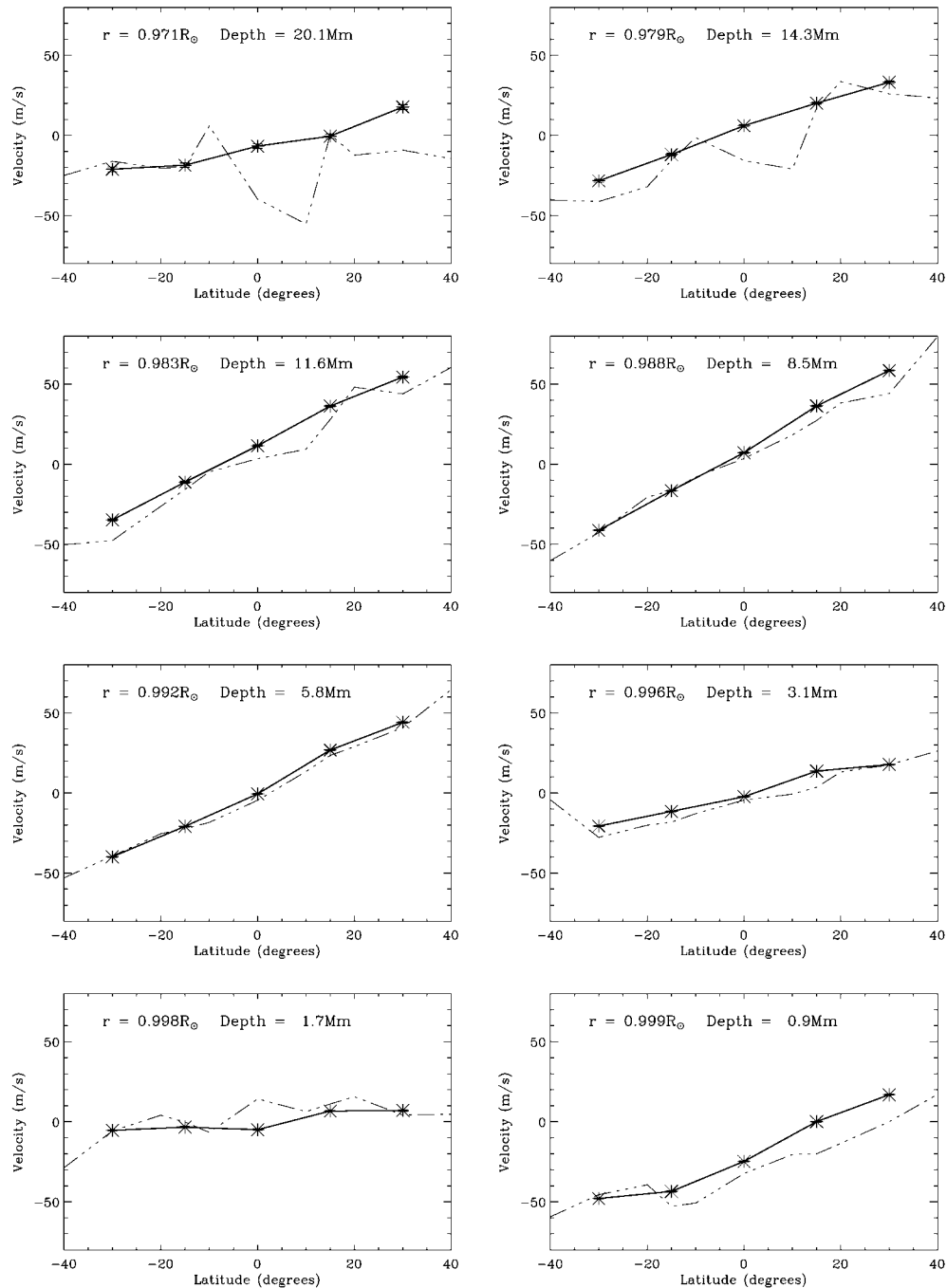


FIG. 3.—Meridional component (U_r) of the horizontal velocity flows at different latitudes. Each curve shows the average results of the 24 sections situated at the same latitude (0° , $\pm 15^\circ$, and $\pm 30^\circ$) at a specific depth. The previous results for 26 sections dispersed in latitude but concentrated in two longitudes (90° and 105°) are overlotted with a dashed line.

REFERENCES

- Arévalo, M. J., Gómez, R., Vázquez, M., Balthasar, H., & Wöhl, H. 1982, *A&A*, 111, 266
 Bahcall, J. N., & Ulrich, R. K. 1988, *Rev. Mod. Phys.*, 60, 297
 González Hernández, I. 1998a, Ph.D. thesis, Univ. La Laguna
 González Hernández, I., Patrón, J., Bogart, R. S., & The SOI Ring Diagram Team. 1998b, in *Structure and Dynamics of the Interior of the Sun and Sun-like Stars*, ed. S. G. Korzennik & A. Wilson (ESA SP-148; Paris: ESA)
 González Hernández, I., Patrón, J., Chou, D.-Y., & The TON Team. 1998c, *ApJ*, 501, 408
 Haber, D. A., Toomre, J., Hill, F., & Gough, D. 1995, in *ASP Conf. Ser. 76, GONG 494: Helio- and Astero-Seismology from the Earth and Space*, ed. R. Ulrich, E. J. Rhodes, Jr., & W. Dappen (San Francisco: ASP), 272
 Hill, F. 1988, *ApJ*, 333, 996
 Patrón, J. 1994, Ph.D. thesis, Univ. La Laguna
 Patrón, J., Hill, F., Rhodes, E. J., & Korzennik, S. G. 1995, *ApJ*, 455, 746
 Pérez Gardé, M. 1979, Ph.D. thesis, Univ. La Laguna
 Scherrer, P. H., et al. 1995, *Sol. Phys.*, 162, 129
 Snodgrass, H. B. 1984, *Sol. Phys.*, 94, 13